



Lower mineralizability of soil carbon with higher legacy soil moisture

Srabani Das^a, Brian K. Richards^a, Kelly L. Hanley^b, Leilah Krounbi^b, M.F. Walter^a,
M. Todd Walter^a, Tammo S. Steenhuis^a, Johannes Lehmann^{b,c,*}

^a Biological and Environmental Engineering, Cornell University, Ithaca, NY, 14850, USA

^b Soil and Crop Sciences, School of Integrative Plant Science, Cornell University, Ithaca, NY, 14850, USA

^c Atkinson Center for a Sustainable Future, Cornell University, Ithaca, NY, 14850, USA

ARTICLE INFO

Keywords:

Soil moisture
Soil organic matter
Stabilization
Turnover

ABSTRACT

The effect of long-term versus short-term water content on soil organic carbon (SOC) mineralizability was evaluated in a six-week incubation trial. Soils were sampled from field sites in upstate New York used for rain-fed bioenergy crop production: nitrogen (N)-fertilized reed canarygrass, switchgrass, switchgrass + N, as well as a broadleaf-grass fallow. Within each cropping system, natural moisture gradients due to topography and subsoil structure allowed us to sample across regions with high (0.5 g g^{-1}), mid (0.4 g g^{-1}) and low (0.3 g g^{-1}) water content. Moisture of the laboratory incubations was adjusted mimicking the three average field moisture levels in a full factorial design. Increasing laboratory moisture in the incubations increased cumulative carbon mineralization per unit soil (C mineralization) and cumulative C mineralization per unit SOC (C mineralizability) (main effect $p < 0.0001$), indicating that lower average moisture as found at this site on average limited mineralization but higher average moisture did not. C mineralizability at high field moisture was 31% (25–42%) lower than at low field moisture across all cropping systems, regardless of moisture adjustment in the incubation. The mean slow C pool size of soils from high field moisture sites ($997.1 \pm 0.1 \text{ mg C g}^{-1} \text{ C}$) was 0.2% greater than that of soils from low field moisture sites ($p < 0.0001$), obtained by fitting a double-exponential model. The mean residence time of the slow mineralizing C pool for soils from low field moisture sites was 5.5 ± 0.1 years, in comparison to 8.0 ± 0.1 years for soils from high field moisture sites ($p < 0.0001$). While permanganate-oxidizable carbon (POXC) per unit SOC ($r = 0.1$) was positively correlated to C mineralizability, wet aggregate stability ($r = -0.2$) was negatively correlated to C mineralizability. Above-ground biomass did not affect C mineralizability ($p > 0.05$) and root biomass marginally influenced ($p = 0.05$) C mineralizability after correcting for soil texture variations. Additionally, after correcting for soil texture variations and biomass inputs, C mineralizability significantly decreased with higher field moisture ($p = 0.02$), indicating possible stabilization mechanisms through mineral interactions of SOC under high water content. Bulk contents of pedogenic iron and aluminum determined by oxalate extraction did not clearly explain differences in mineralizability. However, exchangeable calcium and magnesium contents were significantly ($p < 0.0001$) greater in high moisture soils than soils with low moisture. Additionally, cumulative C mineralizability at 6 weeks was negatively correlated to calcium ($r = -0.7$) and magnesium ($r = -0.6$) and mean residence time of the modeled slow pool correlated positively with calcium ($r = 0.4$). Therefore, cation bridging by retained or illuviated base ions was more important than redox changes of iron as a stabilization mechanism in this experiment.

1. Introduction

Soil moisture is a key environmental control of plant growth and microbial activity, affecting both organic carbon (C) inputs and CO_2 outputs of soil. Globally, soil organic C (SOC) stocks are positively correlated with mean annual precipitation and negatively correlated with mean annual temperature (Trumbore, 1997; Jobbágy and Jackson, 2000). Poorly drained soils usually display higher SOC in comparison to

well-drained soils, especially in temperate ecosystems. While initial decomposition rates of plant residues in surface soils correlate with chemical properties of plant materials such as the C:N ratio or lignin content, it is now understood that long-term stabilization of SOM is an ecosystem property (von Lützow et al., 2006; Schmidt et al., 2011; Stockmann et al., 2013), under the control of parameters such as soil moisture. Soil moisture, temperature, pH, inorganic nutrients, texture and porosity of soil also impact organic matter decomposition or

* Corresponding author. Soil and Crop Sciences, School of Integrative Plant Science, Cornell University, Ithaca, NY, 14850, USA.

E-mail address: CL273@cornell.edu (J. Lehmann).

<https://doi.org/10.1016/j.soilbio.2018.12.006>

Received 27 July 2018; Received in revised form 4 December 2018; Accepted 6 December 2018

Available online 07 December 2018

0038-0717/ © 2018 Elsevier Ltd. All rights reserved.

Table 1
Soil properties of the four cropping systems characterized by high, medium (mid) and low field moisture. Mean values (n = 3) are shown with standard deviations in parenthesis. Letters show significant differences.

	SOC (g kg ⁻¹ soil)			TN (g kg ⁻¹ soil)			Wet aggregate stability (%)			Sand (%)			Silt (%)			Clay (%)			POXC (mg C kg ⁻¹ soil)			POXC per unit SOC (mg C g ⁻¹ C)			pH			
	High	Mid	Low	High	Mid	Low	High	Mid	Low	High	Mid	Low	High	Mid	Low	High	Mid	Low	High	Mid	Low	High	Mid	Low	High	Mid	Low	
Fallow	40.7 (2.4)	38.3 (2.3)	33.9 (1.4)	3.9 (0.6)	3.6 (0.2)	3.2 (0.2)	81.8 (6.4)	76.0 (4.1)	81.8 (6.9)	11.4 (4.0)	14.2 (1.9)	17.5 (1.5)	71.9 (1.7)	66.7 (5)	65.1 (2.1)	16.7 (5.5)	18.9 (4.2)	17.4 (1.5)	87.8 (134)	926 (67)	751 (52)	22 (4.2)	24.2 (2)	22.2 (1)	6.2 (0.1)	6.2 (0.3)	6.1 (0.5)	
Reed cernary grass + N	36.9 (0.6)	36. (5.2)	30.8 (7.4)	3.6 (0.5)	3.5 (0.4)	2.8 (0.5)	63.1 (24)	62.6 (20.3)	60.4 (8.8)	15.2 (0.3)	18.4 (2.5)	18.7 (1.8)	68.6 (5)	66.5 (2.5)	66.6 (0.7)	16.2 (5)	15.1 (1.9)	14.6 (1)	851 (42)	829 (103)	684 (89)	23 (1.2)	23 (2)	23 (4)	5.6 (0.5)	5.6 (0.5)	5.1 (0.1)	
Switch grass	39 (11.5)	29.8 (4.3)	27.9 (3.3)	4.0 (1.2)	2.9 (0.5)	2.7 (0.2)	72.3 (9.3)	59.0 (16.5)	70.5 (22)	11.8 (4.2)	17.2 (4.6)	19.6 (1.4)	68.9 (0.6)	66.8 (0.7)	64.5 (2.5)	19.7 (4.5)	16.0 (5.2)	15.9 (2.1)	827 (41)	762 (84)	613 (111)	22 (5)	26.1 (6)	22 (2)	6.2 (0.5)	6.2 (0.6)	5.8 (0.5)	
Switch grass + N	40.5 (9.8)	26.5 (4.6)	28.8 (0.6)	4.0 (0.7)	2.6 (0.3)	2.9 (0.1)	71.2 (9.5)	54.7 (9.2)	71.7 (20)	15.8 (4.6)	15.8 (1)	23.2 (4.2)	70.0 (2.2)	68.6 (2.8)	62.1 (3.6)	14.2 (2.7)	15.6 (2)	14.7 (1.6)	876 (119)	625 (221)	687 (47)	22.1 (3)	23.1 (5.1)	24 (1.1)	6.3 (0.2)	5.8 (0.1)	5.7 (0.3)	
P value for cropping system	0.1			0.5					0.05	0.06			0.8			0.2			0.08		0.9							0.007

heterotrophic (microbial) respiration.

Hypotheses such as the 'regulatory gate hypothesis' suggest that the limiting step of C mineralization is controlled by abiotic processes which involve conversion of non-bioavailable SOC to bioavailable forms, regardless of microbial biomass or community composition (Kemmitt et al., 2008), which may be impacted by moisture levels in soil. Soil mineralogy plays a key role in determining the amount of SOC and its residence time, especially the slow cycling pool. Torn et al. (1997) showed that the presence of non-crystalline minerals increased along a precipitation gradient and resulted in increased turnover time of stored C. The formation of mineral-organic associations (MOAs) has been recognized as an important mechanism of C stabilization and storage in recent decades (Kleber et al., 2015). Iron (Fe) and aluminum (Al) minerals play a key role in SOC stabilization (Kögel-Knabner et al., 2008) and can be predictors of SOC storage in soils with high extractable metals in moderately acidic to circumneutral pH (Porrás et al., 2017). Kleber et al. (2005) observed a significant positive correlation between SOC and oxalate extractable Fe in acid soils. The importance of polyvalent cations in SOC stabilization shifts from Al to Fe to calcium (Ca) as soil pH moves from acidic to basic conditions (Tipping, 2005; Rowley et al., 2018). Calcium is well known to be related to SOC interactions, and Ca-facilitated SOC stabilization mechanisms are well characterized (Rowley et al., 2018). Calcium plays an important role in SOC accumulation of various ecosystems in temperate latitudes, pastures (Fornara et al., 2011), and restored prairies (O'Brien et al., 2015). Calcium and magnesium (Mg) promote clay flocculation and bind organic matter to clay surfaces through electrostatic interactions, thus reducing microbial breakdown of OM (Kögel-Knabner et al., 2008). Cations such as Ca and clay minerals also interact with OM to form nanometer-to micrometer-sized structures which aid SOC stabilization (Chenu and Plante, 2006; Rowley et al., 2018).

Updated concepts of SOC stabilization, such as the soil continuum model (SCM), focus on spatial arrangement of soil organic matter and controls of temperature, moisture and soil mineralogy. The spatial arrangement of OM within the mineral matrix, micro-redox environment, microbial ecology and interaction with mineral surfaces, all factors contributing to OM persistence in the SCM model are impacted by moisture independently as well as through moisture-temperature interactions (Lehmann and Kleber, 2015). Several SOC models typically use soil moisture-respiration functions representing the average response of microbial respiration to soil moisture contents, but information about variations in response to different stabilization mechanisms because of different moisture contents is lacking. Hence, it is important to understand the impact of legacy soil moisture effects on the respiration-moisture relationship. This may affect C mineralizability that is commonly used in C simulation models (Kirschbaum, 2006).

The objective of this study was to provide a mechanistic understanding of the long-term role of moisture on SOC mineralizability and stabilization. We investigated whether any or all the following legacy effects from different field moisture levels determined C mineralizability with varying moisture contents: (1) plant above-ground/below-ground biomass inputs and therefore SOC contents; (2) SOC stabilization and therefore the extent of mineral protection of SOC; and (3) SOC accumulation due to lower mineralizability because moisture-mineralization relationships change because of different SOC contents or forms. We hypothesized that those soil moisture contents that result in the lowest mineralization and highest plant growth also generate the greatest SOC accrual.

2. Materials and methods

2.1. Experimental site

The field site located near Ithaca, New York, USA (42N28.20', 76W25.94'; Fig. S1), encompassed three primary soil series: well-drained Canaseraga (coarse-silty, mixed, active, mesic typic

Fragiudept), somewhat poorly drained Dalton (Coarse-silty, mixed, active, mesic aeris Fragiuaquept) and poorly drained Madalin (fine, illitic, mesic mollic Endoaqualf). The epipedon texture is primarily silt-loam. The different soil properties are shown in Table 1. The field topography is undulating, with slopes in the sampled areas varying from 0 to 8% (and a small area with short slopes up to 15% on the eastern edge). Perched water tables resulting from shallow restrictive layers recur seasonally where lateral interflow creates saturated depressions (Steenhuis et al., 1995; Zollweg et al., 1996; Walter et al., 2000). The field is marginal for row crop or alfalfa production (Richards et al., 2014) due to wetness. Perennial grasses were established in July 2011, before which the field had been fallow for circa 50 years, with occasional mowing. The mean annual temperature and precipitation at the site are 10 °C and 940 mm, respectively.

2.2. Field experiment

A randomized complete block design was used for 16 large strip-plots (denoted A through P, Fig. S1) that comprised four replicate plots of each of four cropping treatments: switchgrass (*Panicum virgatum* L. Shawnee), switchgrass + nitrogen (N) fertilizer, reed canarygrass (*Phalaris arundinaceae* L. Bellevue) + N and pre-existing fallow control (Fallow). Where used, the N fertilization rate was 74 kg N ha⁻¹, surface-applied as ammonium sulfate ((NH₄)₂SO₄). Fertilization started in spring 2012 for reed canarygrass + N and in spring 2013 for switchgrass + N.

Five sub-plots were established along the natural moisture gradients of each strip-plot (Fig. S1), varying from moderately well-drained to poorly-drained due to topography and shallow restrictive layers (Das et al., 2018). Moisture measurements commenced in summer 2011 and continued throughout the experiment. The volumetric water content (VWC) was measured using time-domain reflectometry (TDR) soil moisture sensor with 0.12 m probes (Hydrosense™, Campbell Scientific Australia Pty. LTD.). The TDR instrument was used to determine soil moisture from the average of 3 measurements taken at each sub-plot. The subplot approach thus yielded 80 permanent sampling points where frequent periodic water content measurements were used to characterize the relative soil moisture status of each subplot. For each measurement event, a field average volumetric water content of all 80 subplots was calculated, and each subplot's value was normalized relative to the field mean (yielding a “relative soil moisture ratio” for that subplot and time point) (Richards et al., 2013). These relative values were averaged over the entire study period for each subplot and each subplot's characteristic wetness (relative to the field average) was thus established over 40 such measurement events cumulatively representing several thousand readings at the site.

The multi-year mean values for the 80 subplots were aggregated into “soil wetness quintiles” for each treatment for the entire study period. The VWC values were then converted to the proportion of water filled pore space (WFPS) by scaling the instrument's values based on a linear trend that was established from the average VWC observed for saturated (100% WFPS) and dry (0% WFPS) conditions (Mason et al., 2017). Instantaneous values of WFPS at each subplot were further converted to ratios of the simultaneous field average. A long-term wetness ranking was established, similar to the VWC ranking technique. The WFPS values corresponding to long-term VWC quintile 1 (high), quintile 3 (mid) and quintile 5 (low) were 63%, 50% and 40% respectively. Additionally, VWC was related to the gravimetric water content (Fig. S2), to compute mean water content values corresponding to the long-term high, mid and low VWC quintiles from the field. The mean gravimetric water content corresponding to quintile 1 (high), quintile 3 (mid) and quintile 5 (low) were 0.5, 0.4, and 0.3 g g⁻¹ respectively (Table S1).

2.3. Field sampling protocol

For the incubation, soils from subplots wetness quintiles were randomly chosen (Table S1). Soil from the Ap horizon was sampled in August 2014, after more than a week without rain, and three months after N fertilization. A flat shovel was used to dig to a depth of 0.15 m (defined here as the average Ap horizon) at two locations equidistant (1.2 m) from the center of each subplot (as marked by a permanent subplot flag). Approximately 2 kg of soil was dug from each of the two locations, composited in a bucket, and thoroughly mixed. Subsamples of ~200 g were then transferred to labeled polyethylene bags stored in a portable cooler. At the time of sampling, VWC was also determined.

2.4. Laboratory analyses of soil and crop parameters

The gravimetric water content of soil samples was determined by weighing 10 g of soil and drying at 105 °C for 24 h and reweighing (Jarrell et al., 1999). Elemental C and N analysis of oven dried (60 °C) soils was carried out by combustion infrared detection [LECO TruMac CN, LECO Corp, St. Joseph, MI, precision-Nitrogen-0.01 mg or 0.3% RSD (whichever is greater) and Carbon- 0.01 mg or 0.4% RSD (whichever is greater)]. Soil pH and texture analyses were performed as per Moebius-Clune et al. (2016). As all soil pH values were below 7, we assumed carbonate was not present, and equated total C to SOC (Propheter and Staggenborg, 2010; Bonin and Lal, 2014). This was further confirmed on a subset of 16 soil samples by the lack of effervescence following treatment with 5 M HCl.

Permanganate-oxidizable carbon (POXC) was determined via permanganate oxidation and spectrophotometry (Weil et al., 2003; Culman et al., 2012; Moebius-Clune et al., 2016). The stability of soil aggregates between 0.25 mm and 2 mm (wet aggregate stability) was measured using a sprinkle infiltrometer (Moebius-Clune et al., 2016). Fe (Fe_o) and Al (Al_o) oxides (the o subscript denotes acid ammonium oxalate-extractable Fe and Al) were measured by selective dissolution with acid ammonium oxalate in darkness, using a modification of the procedure of Schwertmann (1964) and McKeague and Day (1966). Oxide concentrations were determined using an inductively coupled plasma atomic emission spectrometry (iCAP 6000 series ICP spectrometer, Thermo Scientific, Waltham, MA). Ca and Mg were extracted from soil by shaking with Modified Morgan's solution (ammonium acetate and acetic acid solution buffered at pH 4.8) using a procedure adapted from Sposito et al. (1982). After shaking and filtration, filtrates were analyzed on an inductively coupled plasma emission spectrometer (ICP, Spectro Arcos) as outlined in Moebius-Clune et al. (2016).

Above-ground biomass yields from each subplot were determined for the years 2012, 2013 and 2014 using hand-harvesting of replicate 1 m² quadrants, weighing, and dry matter analysis. Values from the three years were subsequently added to obtain cumulative harvested above-ground biomass (harvestable standing biomass). We did not use the 2011 baseline (pre-establishment) biomass from the field for this calculation. Root biomass was determined gravimetrically. First, coarse roots were removed from 60 °C oven-dried soil samples by hand picking (root crowns were not sampled). Roots were then passed through a 2 mm-sieve and weighed. Even though this dry separation procedure removed all visible soil, it may still be contaminated with soil material and therefore constitute an overestimate; albeit differences between the plots remain valid, as we do not expect systematic bias since samples were dried before separation. The coarse root biomass estimation from each subplot for the third year was undertaken in 2014 and used for analysis. The cumulative harvestable above-ground biomass (2012–2014) and standing root biomass (2014) are shown in Table 2.

2.5. Incubation experiment

Field-moist soils were passed through a 4-mm sieve to remove plant roots and rocks. Samples were then split into two batches, one for the

Table 2

Cumulative above-ground harvestable biomass (2012–2014) and standing root biomass (2014) from four cropping systems characterized by high, medium (mid), and low field moisture. Mean^a values (n = 3) are shown with standard deviations in parenthesis. Letters show significant differences.

	Cumulative above-ground harvestable biomass (Mg ha ⁻¹)			Root biomass (g kg ⁻¹ soil)		
	High	Mid	Low	High	Mid	Low
Fallow	12 a (1.7)a	11 a (2.4)	13 a (1.4)	13.1 a (3.6)	5.9 b (4.5)	10 a (1.9)
Reed canarygrass + N	12.3 a (0.3)	13.1 a (2.2)	12.4 a (4.6)	12.7 a (3.7)	6.8 b (2.1)	6.3 b (4.1)
Switchgrass	8.5 b (3.5)	12.2 b (6.4)	19.3 a (5.4)	4.1 a (1.3)	2 b (0.7)	3.3 ab (1.8)
Switchgrass + N	9.6 b (3)	10.4 b (1.9)	18.1 a (3.3)	7.9 a (2.6)	4.7 b (2.2)	3 b (2.3)
P value for cropping system	0.7			< 0.0001		

^a Low above-ground biomass can be explained with the early phase of crop establishment on soils with comparably high moisture levels in comparison to high root biomass that likely also remained from preceding fallow vegetation and may contain some mass contamination from adhering mineral soil (see Methods).

incubation experiment, and the other for determining gravimetric water content and soil properties. 15 g of field moist soil were transferred into pre-weighed 60-mL glass Qorpak vials for the incubation experiment and were then air dried for 48 h at 30 °C in a climate-controlled incubation chamber, where the samples were kept for the duration of the experiment. Air-dried soil samples were then adjusted to long-term equivalent levels of high, mid and low gravimetric (0.5, 0.4 and 0.3 g⁻¹ g respectively) field moisture contents before incubation. Two technical replicates (duplicates) were set up for each moisture adjustment.

The incubation set-up consisted of a full factorial design of four cropping systems by three field replicates by three field water contents (high, medium (mid), and low) by three laboratory water contents (high, mid, and low) in duplicates (technical replicates that were not used in the statistical analysis). The Qorpak vials were transferred to 473-mL wide-mouth Mason jars. A 20-mL scintillation vial containing freshly prepared 15-mL 0.09M KOH was also placed open in the Mason jar and the jar was then capped tightly. The KOH solution used to trap CO₂ emitted was prepared with CO₂-free deionized water (DIW) (Whitman et al., 2014). For every 12 samples, 1 blank was used. The blank sample set-up consisted of only a KOH trap in the Mason jar and no soil addition. The incubation was carried out in the dark.

A staggered sampling schedule for CO₂ measurements was used due to the high number of sample vials (216). Three batches of 72 samples consisting of duplicates of each wetness level and six blanks were established for measuring one batch on a single sampling day. On days 1, 3, 7, 14, 21, 28, and 42 for each batch, the jars were opened and the electrical conductivity (EC) of the KOH traps was measured at a constant temperature of 30.0 (± 3) °C. Fresh vials of 15 mL 0.09M KOH then replaced the previous ones, and the Mason jars were resealed. With each measurement of electrical conductivity, the soil-containing Qorpak vials were weighed and the water content in the soil was readjusted to its designated wetness level by addition of DIW as needed. The maximum CO₂ capture of the 0.09M KOH was kept below 60% of its saturation.

On one of the sampling days, a standard curve was established by sealing KOH traps in Mason jars with rubber septa in their lids and injecting a known volume of CO₂. The EC of the traps was measured after 24 h and linearly correlated with the known CO₂ volumes to create a standard curve (Fig. S3). To account for the small amount of background atmospheric CO₂ present in the jar, EC measurements from the

'blank' from each group was subtracted from that of each sample jar. The resulting delta EC value was then converted into total CO₂ released by the sample using the standard curve (Fig. S3). The CO₂ units were converted to gravimetric units of C using the universal gas law equation. The resulting CO₂ emission was then normalized for per g soil or per g SOC. For the latter, results were divided by the amount of SOC present in the soil at the beginning of the incubation. Cumulative C mineralization was calculated for each replicate soil obtained from different field plots (after averaging the two analytical duplicates from the same field plot), and averages were computed for each cumulative dataset.

2.6. Statistical analyses and modeling

SOC mineralization data were fitted to a double exponential model, based on the highest r square values (r² > 0.99) during pre-analysis. The mean cumulative mineralization value for three field replicates of each field-lab moisture combination was fitted with a first-order, two-pool model (Liang et al., 2008; Zimmerman et al., 2011). Data were fitted in nlsLM (nonlinear regression, Levenberg-Marquardt search), R Studio Team (2015). The Levenberg-Marquardt algorithm estimates the values of the model parameters to minimize the sum of the squared differences between model-calculated and measured values.

$$C_{\text{cumulative}} = C_1 (1 - e^{-k_1 t}) + C_2 (1 - e^{-k_2 t})$$

Where, C_{cumulative} is CO₂-C production per unit soil (mg C g⁻¹ soil), t is time in days, C₁ is the fast mineralizing soil carbon pool, C₂ is the slow mineralizing soil carbon pool, and k₁ and k₂ are the first-order decomposition rate coefficients for fast and slow pools, respectively. Parameter constraints were chosen as follows: k₁ > 0, k₂ > 0 and C₁ + C₂ = initial SOC in the soil sample expressed as mg g⁻¹ soil. Curve fitting was also done using the same equation for CO₂-C production per unit initial SOC (mg C g⁻¹ C) with parameter constraints chosen as k₁ > 0, k₂ > 0 and C₁ + C₂ = 1000 mg C. We also assigned a fixed value of k₁ and performed curve fitting to address over-parameterization of the model and to obtain better estimates of the slow mineralizing pool dynamics (Table S6). The results were near identical (r² = 0.68, slope of 0.94 for C₂ and r² = 0.81, slope of 0.97 for k₂). The same result was observed if both k₁ and C₁ were fixed to an average value (data not shown).

A three-way ANOVA was performed using cumulative C mineralization per unit SOC (from here on called "C mineralizability") and per unit soil (called "C mineralization") at 42 days, with fixed effects of field moisture level, laboratory moisture level, and cropping system. An ANOVA was also performed for the three parameters estimated by the double exponential model.

The three-way interaction between field moisture level, laboratory moisture level, and cropping system and the two-way interaction between laboratory moisture level vs cropping system was not found to be significant (p value > 0.05) in all models. Thus, only the two-way interactions between field moisture level and laboratory moisture level and field moisture level vs cropping system were considered in the final models. Multiple comparison of Least Square Means differences was conducted only when the ANOVA results for the main effects or interactions were significant. Post-hoc comparisons were made using Tukey's HSD method to control for multiple comparisons. Five jars out of 216 were excluded due to suspected leaks (strong outliers, 6–8 standard deviations from all samples).

To explore the primary factors influencing C mineralizability, we performed a series of statistical analyses. First, univariate analyses allowed us to establish the soil property variables significantly correlated with C mineralizability. Pearson correlation coefficients were computed between cumulative C mineralizability (mg C g⁻¹C) and SOC, total nitrogen (TN), POXC, POXC per unit SOC, wet aggregate stability, soil texture, soil pH, Fe_o, Al_o, Ca, Mg, cumulative harvested above-ground

biomass, and root biomass in 2014.

To address collinearity among soil properties influencing C mineralizability, we then performed principal components analysis (PCA) for the dataset (adding POXC per unit SOC and excluding soil texture). To identify the control of soil texture and biomass inputs on C mineralizability, we performed a mixed effects model analysis with the first two principal components, field and laboratory moisture levels, above-ground and root biomass, sand and clay content as fixed effects and subplots as random effects. Thus, the significance of moisture in influencing C mineralizability, when corrected (controlled) for biomass inputs and soil texture, was tested. Additionally, a principal components analysis for the dataset including C mineralizability and all correlated variables was performed. The bi-plot report the eigenvectors and proportion of variance explained by the first two principal components. The variables included in the analysis were plotted as vectors representative of the strength and direction to which they loaded each component. Statistical analyses were carried out using JMP Pro 12 (SAS Inc., Cary, NC).

3. Results

3.1. C mineralization and C mineralizability

While higher laboratory moisture, averaged over cropping systems and field moisture, significantly ($p < 0.0001$, Fig. 1a, Table S2a) increased cumulative CO_2 evolution per unit soil mass (C mineralization) at 42 days, field-moisture, averaged over cropping system and laboratory moisture, did not have a significant effect ($p = 0.7$, Fig. 1a, Table S2a). Additionally, cropping system, averaged over field and laboratory moisture, had a significant ($p = 0.005$, Fig. 1a, Table S2a) effect on C mineralization, with C mineralization in fallow plots being greater than that in switchgrass plots (Table S2b). The interaction between field moisture level and lab moisture adjustment had a significant effect on C

mineralization ($p = 0.001$, Table S2a). When expressed as cumulative CO_2 evolution per unit SOC (C mineralizability) at 42 days, high ambient field moisture had the lowest values for all laboratory moisture adjustments and cropping systems (Fig. 2a–d). Furthermore, high field moisture resulted in significantly ($p = 0.002$) lower C mineralizability than low field moisture levels (Fig. 1b, Tables S3a and S3b), when averaged over cropping systems and laboratory adjustments. Higher laboratory moisture averaged over cropping systems and field moisture levels, significantly ($p < 0.0001$, Fig. 1b) increased C mineralizability, with lab-high being significantly greater than lab-low. The interactions between field moisture and cropping system and between field moisture level and laboratory moisture adjustment were not significant ($p > 0.05$). The moisture combination of field-high and lab-low had the lowest value in each of the cropping system soils (Fig. 2).

The size of slow mineralizing C pool (C_2) varied between 993.2 ± 0.0 and $997.9 \pm 0.1 \text{ mg C g}^{-1} \text{ C}$ among various moisture-crop combinations (Table 3). Field moisture level ($p < 0.0001$), laboratory adjustment ($p < 0.0001$) and the interaction between field moisture and cropping system (0.0002) were significant for explaining variations of C_2 (Table S4a). The size of C_2 was greatest for soils with a combination of field-high and lab-low moisture compared to other moisture levels, regardless of the cropping system (Table 3). Fixing the rate of mineralization at an average value of k_1 (Table S6) did not significantly change C_2 or k_2 ($r^2 = 0.69$ and $r^2 = 0.82$, respectively).

The mineralization rate constants of the slow degrading pool (k_2 , 0.00024 ± 0.000 to 0.00064 ± 0.000) were three orders of magnitude lower than those of the fast degrading pool (k_1 , 0.1 ± 0.003 to 0.58 ± 0.005). The mean residence time of the fast mineralizing pool (MRT_1) varied between 2.1 ± 0.1 and 6.1 ± 0.6 days and that of the slow mineralizing pool (MRT_2) varied between 4.3 and 11.2 years among the different moisture-crop combinations (Table 3).

While the MRT_2 of soils from high field moisture was significantly greater ($p < 0.0001$) than that of soils from mid or low field moisture,

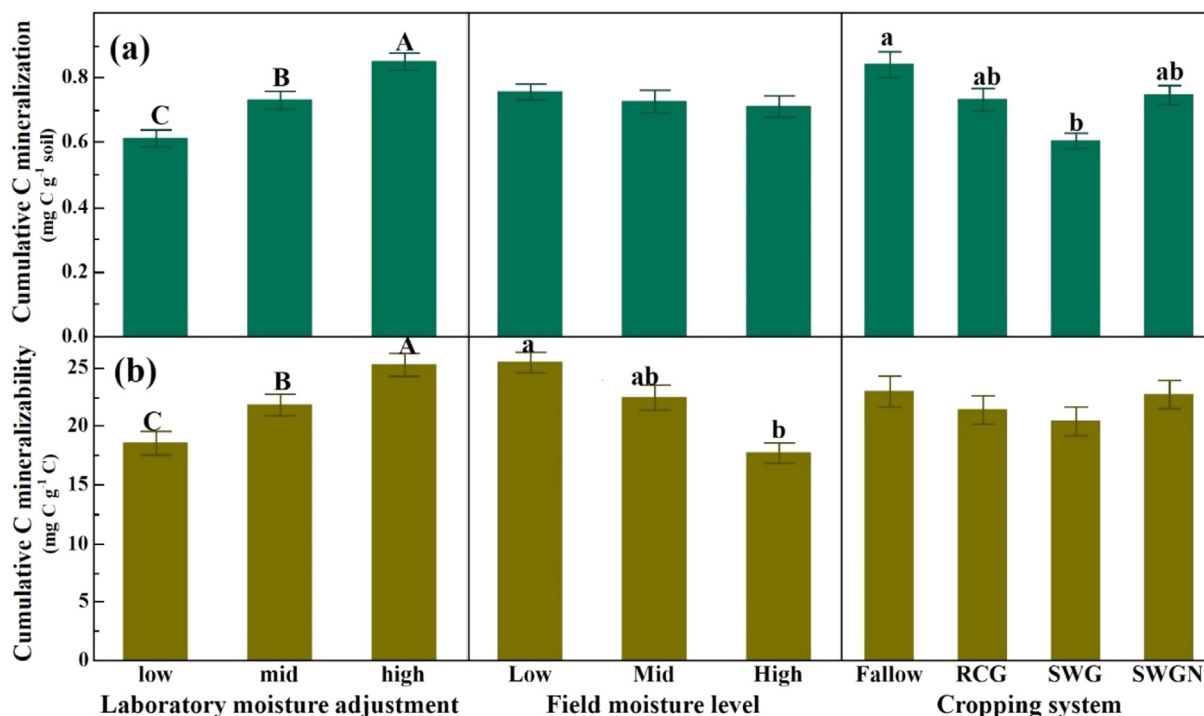


Fig. 1. Mean cumulative C mineralization (a) and C mineralizability (b) after 42 days. Different letters above bars indicate significant differences within the same figure panel ($p < 0.05$). Mean laboratory moisture values (mean + SE, $n = 36$, each averaged over 2 technical replicates) are averaged over field moisture and cropping systems, mean field moisture values (mean + SE, $n = 36$, each averaged over 2 technical replicates) are averaged over laboratory moisture and cropping systems and mean cropping system values (mean + SE, $n = 27$, each averaged over 2 technical replicates) are averaged over field moisture and laboratory moisture. The cropping systems were fallow-control (fallow), reed canarygrass + fertilizer 75 kg N ha^{-1} (RCGN), switchgrass (SWG) and switchgrass + fertilizer 75 kg N ha^{-1} (SWGN).

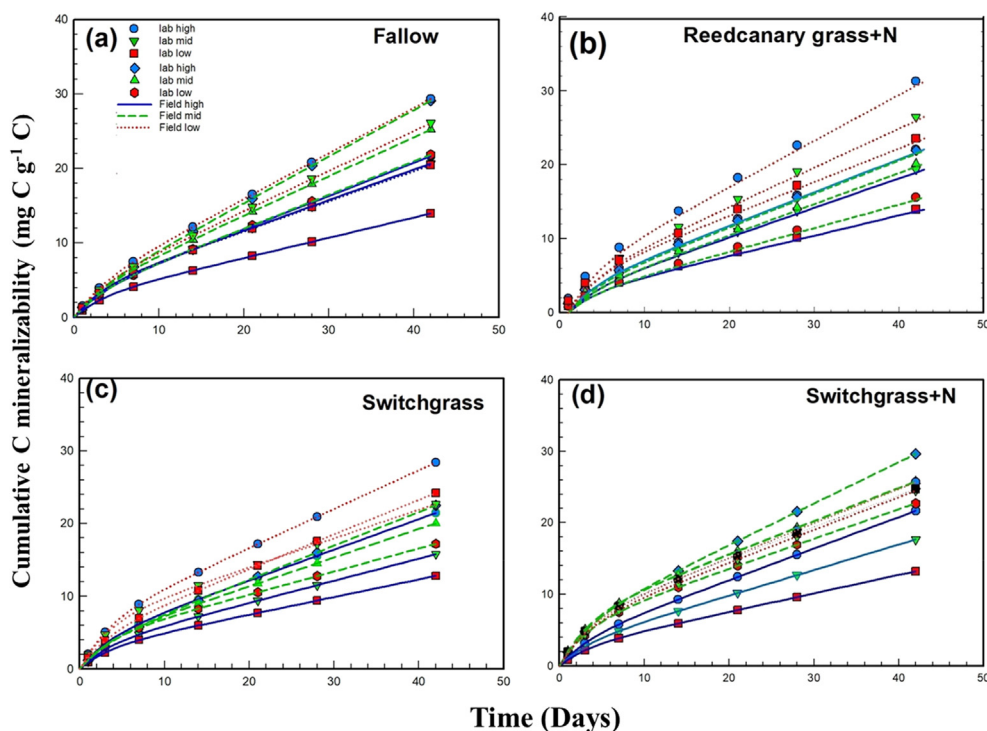


Fig. 2. Cumulative C mineralizability over time in soils subjected to variable lab moisture regimes, per each field moisture regime and cropping system (Mean + SE, $n = 3$ replicates averaged over 2 technical duplicates); fallow-control (a), reed canary-grass + fertilizer 75 kg N ha^{-1} (b), switchgrass (c) and switchgrass + fertilizer 75 kg N ha^{-1} (d). Lines are a fit using a double-exponential model, the parameters of which are presented in Table S6.

MRT₂ of soils adjusted to low laboratory moisture was significantly greater ($p < 0.0001$) than that of soils adjusted to mid and high laboratory moisture conditions (Table S5a). The interactions between field moisture level and cropping system ($p = 0.01$) and field moisture level and laboratory moisture adjustment ($p = 0.0001$) were also significant (Fig. 3, Tables S5a, S5c, S5d).

3.2. Soil properties, oxalate-extractable Fe/Al oxide and acetate extractable Ca/Mg of soils of different field moisture levels

Texture for soils from the 36 sub plots was relatively uniform (sand $16.6\% \pm 4$, silt $67.2\% \pm 3.5$, clay $16.2\% \pm 3.3$) with no significant texture difference among the soils of the three wetness groups from the different cropping systems. Nevertheless, to understand the influence of moisture on C mineralization, we used soil texture as a fixed effect, in the model predicting the impact of different variables on C mineralization. The soil properties are presented in Table 1.

Fe_o values and combined values of Fe_o and Al_o were not significantly different between the soils of the three moisture classes, while wettest soils had significantly greater Al_o than mid moisture soils (Table 4). However, extractable Ca and Mg were both significantly greater in the wettest soils than in the mid or low moisture soils (Table 4).

3.3. C mineralization and C mineralizability in relation to soil and crop parameters

No correlations were observed between cumulative C mineralization and most soil properties or above-ground biomass. C mineralization was weakly correlated to Ca ($r = -0.2$, $p = 0.02$), Al_o ($r = -0.3$, $p = 0.009$), and root biomass ($r = 0.3$, $p = 0.003$) (Fig. S4a). However, Pearson correlations between cumulative C mineralizability and soil properties or biomass measured at the start of the experiment, before texture corrections, indicated strong negative correlation with SOC ($r = -0.5$, $p < 0.0001$), TN ($r = -0.6$, $p < 0.0001$), Ca ($r = -0.7$, $p < 0.0001$), Mg ($r = -0.6$, $p < 0.0001$), Al_o ($r = -0.5$, $p < 0.0001$), POXC ($r = -0.5$, $p < 0.0001$), and weak negative correlation with soil pH ($r = -0.3$, $p = 0.002$), clay ($r = -0.2$, $p = 0.03$), wet aggregate stability ($r = -0.2$, $p = 0.03$), and root biomass

($r = -0.01$, $p = 0.9$). It also indicated weak positive correlation with sand ($r = 0.26$, $p = 0.01$) and cumulative above-ground biomass ($r = 0.004$, $p = 0.9$) (Fig. S4b).

Modeled MRT₂ showed a positive correlation with Ca ($r = 0.4$, $p = 0.02$), POXC ($r = 0.3$, $p = 0.04$), and a negative correlation with sand contents ($r = -0.5$, $p = 0.006$), whereas modeled C₂ indicated a strong positive correlation with Ca ($r = 0.6$, $p = 0.0003$), Mg ($r = 0.5$, $p = 0.003$), SOC ($r = 0.5$, $p = 0.001$), and a negative correlation with sand contents ($r = -0.4$, $p = 0.01$) and POXC per unit SOC ($r = -0.4$, $p = 0.006$) (data not shown).

For the first principal component (PC1), SOC (0.96), TN (0.96), Ca (0.9), Mg (0.81) Al_o (0.57), wet aggregate stability (0.61), POXC (0.72), and soil pH (0.59) loaded in the same direction, whereas POXC per unit SOC (-0.41) loaded in the opposite direction, which explained 50.5% variability among soil properties (Fig. 4, Tables S7a and S7b). For the second principal component (PC2) which explained 20.4% of variability, soil pH (-0.46), POXC (-0.37) and POXC per unit SOC (-0.59) loaded substantially in opposite direction and Fe_o (0.84) and Al_o (0.72) in the same direction.

PC1 ($p = 0.0008$), field moisture level ($p = 0.02$) and lab moisture level ($p < 0.0001$) were significant in explaining variations in C mineralizability (Table 5). However, PC2, cropping system, cumulative harvested above-ground biomass, sand or clay contents were not significant in explaining variations in cumulative C mineralizability, and 2014 root biomass was marginally important ($p = 0.05$) in controlling C mineralizability. Thus, when controlled for soil texture, cumulative above-ground biomass or 2014 root biomass, field moisture was significant in influencing C mineralizability ($p = 0.02$, Table 5).

For the PCA including C mineralizability and all correlated soil and crop variables (not corrected for soil texture), the eigenvectors and proportion of variance explained by the first two principal components are shown in Fig. S5 and Tables S8a and S8b, respectively.

Table 3

Carbon mineralization kinetics of soil after incubation for 42 days at 25 °C for the different cropping systems (Mean + SE), n = 3 replicates each using technical duplicates, for the three laboratory level adjustments of three field moisture levels of each cropping system). Pool sizes and decay rates of cumulative soil C mineralization per unit SOC using double exponential model $Cumulative = C_1 (1 - \exp(-k_1 x)) + (1000 - C_1) (1 - \exp(-k_2 x))$, where C_1 is the fast pool, C_2 is the slow pool and k_1 and k_2 are the first-order decomposition rate coefficients for fast and slow pool respectively, the parameter constraints chosen, $k_1 > 0$, $k_2 > 0$. MRT_1 is the mean residence time of the fast-mineralizing pool in days ($MRT_1 = 1/k_1$) while MRT_2 is the mean residence time of slow-mineralizing pool in years ($MRT_2 = (1/k_2)/365$). (for calculations using fixed k_1 values, please see [Supplementary Table S6](#)).

Cropping system	Field moisture level	Lab moisture	C_1 (mg C g ⁻¹ C)	k_1 (day ⁻¹)	C_2 (mg C g ⁻¹ C)	k_2 (day ⁻¹)	MRT_1 (days)	MRT_2 (years)
Fallow	high	high	2.9 ± 0.1	0.3 ± 0.00	997.1 ± 0.1	0.00045 ± 0.000	3.4	6.1
	high	mid	5.5 ± 0.5	0.1 ± 0.00	994.5 ± 0.5	0.00036 ± 0.000	8.3	7.7
	high	low	2.3 ± 0.1	0.4 ± 0.01	997.7 ± 0.1	0.00028 ± 0.000	2.6	9.8
	mid	high	3.6 ± 1.1	0.2 ± 0.00	996.4 ± 1.1	0.00061 ± 0.000	6.3	4.5
	mid	mid	4.0 ± 0.8	0.2 ± 0.00	996.0 ± 0.8	0.00051 ± 0.000	5.9	5.4
	mid	low	3.0 ± 0.3	0.3 ± 0.01	997.0 ± 0.3	0.00045 ± 0.000	3.8	6.0
	low	high	3.2 ± 0.2	0.4 ± 0.00	996.8 ± 0.2	0.00064 ± 0.000	2.4	4.3
	low	mid	3.9 ± 0.4	0.2 ± 0.00	996.1 ± 0.4	0.00053 ± 0.000	4.7	5.2
	low	low	3.5 ± 0.2	0.3 ± 0.00	996.5 ± 0.2	0.00041 ± 0.000	3.7	6.7
Reed canarygrass + N	high	high	4.2 ± 0.4	0.17 ± 0.03	995.8 ± 0.4	0.00043 ± 0.000	6.0	6.4
	high	mid	2.8 ± 0.2	0.23 ± 0.03	997.2 ± 0.2	0.00040 ± 0.000	4.4	6.9
	high	low	2.5 ± 0.1	0.26 ± 0.02	997.5 ± 0.1	0.00027 ± 0.000	3.8	10.0
	mid	high	2.7 ± 0.1	0.35 ± 0.03	997.3 ± 0.2	0.00046 ± 0.000	2.9	5.9
	mid	mid	2.5 ± 0.2	0.26 ± 0.05	997.5 ± 0.2	0.00042 ± 0.000	3.9	6.5
	mid	low	2.2 ± 0.2	0.26 ± 0.05	997.8 ± 0.4	0.00032 ± 0.000	3.8	8.6
	low	high	6.1 ± 0.4	0.29 ± 0.04	993.9 ± 0.4	0.00040 ± 0.000	3.4	6.8
	low	mid	4.8 ± 0.4	0.20 ± 0.03	995.2 ± 0.4	0.00052 ± 0.000	4.9	5.3
	low	low	5.0 ± 0.4	0.21 ± 0.03	994.9 ± 0.4	0.00044 ± 0.000	4.8	6.2
Switchgrass	high	high	4.9 ± 0.7	0.16 ± 0.03	995.1 ± 0.7	0.00039 ± 0.000	6.3	7.0
	high	mid	3.1 ± 0.0	0.27 ± 0.07	996.9 ± 0.0	0.00030 ± 0.000	3.7	9.0
	high	low	2.6 ± 0.2	0.29 ± 0.05	997.4 ± 0.2	0.00024 ± 0.000	3.5	11.2
	mid	high	2.8 ± 0.1	0.33 ± 0.03	997.2 ± 0.1	0.00048 ± 0.000	3.0	5.8
	mid	mid	3.3 ± 0.2	0.35 ± 0.04	996.7 ± 0.2	0.00040 ± 0.000	2.9	6.8
	mid	low	4.0 ± 0.3	0.27 ± 0.04	996.0 ± 0.3	0.00031 ± 0.000	3.7	8.7
	low	high	6.1 ± 0.4	0.26 ± 0.04	993.9 ± 0.4	0.00054 ± 0.000	3.8	5.1
	low	mid	6.1 ± 0.4	0.29 ± 0.29	993.9 ± 0.4	0.00040 ± 0.000	3.4	6.8
	low	low	3.6 ± 0.4	0.49 ± 0.15	996.4 ± 0.4	0.00050 ± 0.000	2.0	5.5
Switchgrass + N	high	high	2.6 ± 0.1	0.58 ± 0.05	997.4 ± 0.1	0.00046 ± 0.000	1.7	5.9
	high	mid	2.4 ± 0.3	0.41 ± 0.30	997.6 ± 0.5	0.00037 ± 0.000	2.4	7.4
	high	low	2.1 ± 0.1	0.41 ± 0.10	997.9 ± 0.3	0.00027 ± 0.000	2.4	10.2
	mid	high	5.8 ± 0.5	0.22 ± 0.51	994.2 ± 0.3	0.00057 ± 0.000	4.6	4.8
	mid	mid	6.8 ± 0.6	0.23 ± 0.64	993.2 ± 0.0	0.00045 ± 0.000	4.3	6.0
	mid	low	6.0 ± 0.3	0.21 ± 0.31	994.0 ± 0.2	0.00040 ± 0.000	4.7	6.8
	low	high	5.1 ± 0.4	0.36 ± 0.40	994.9 ± 0.0	0.00050 ± 0.000	2.8	5.5
	low	mid	3.9 ± 0.4	0.21 ± 0.40	996.1 ± 0.4	0.00053 ± 0.000	4.7	5.2
	low	low	3.5 ± 0.2	0.27 ± 0.21	996.5 ± 0.1	0.00041 ± 0.000	3.7	6.7

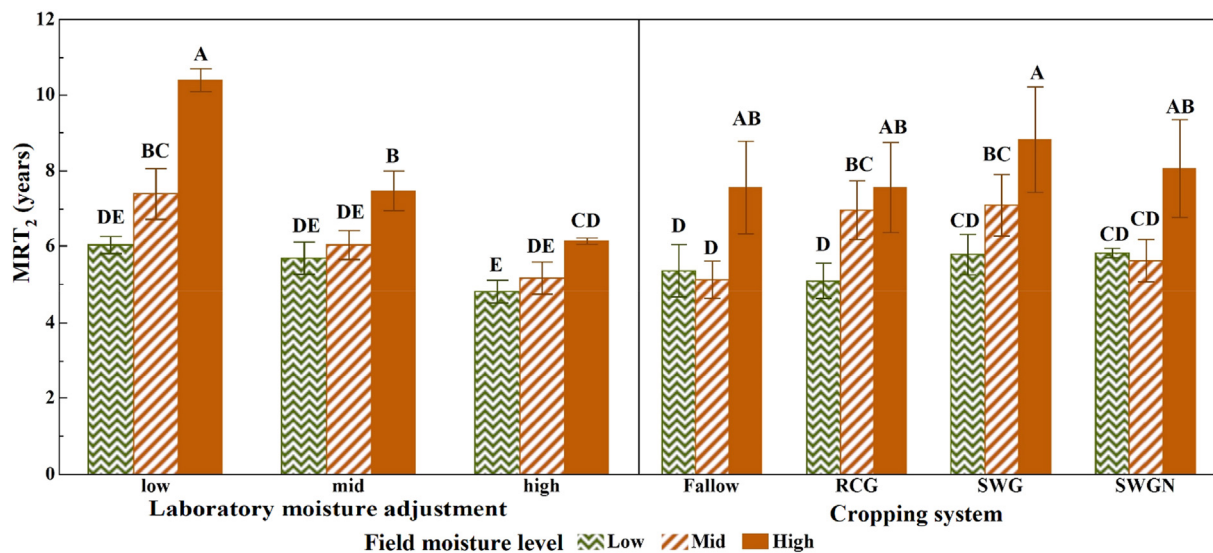


Fig. 3. Mean residence time of slow mineralizing carbon pool (MRT_2) of soils from different laboratory water adjustments and cropping regimes under variable field moisture levels, as modeled with a double-exponential equation, with fixed k_1 of 0.3 (Fig. 2, Table S6). Values are averaged across all field moisture levels (n = 9 replicates each averaged over 2 technical duplicates). Different letters within bars indicate significant differences ($p < 0.05$).

Table 4

Oxalate-extractable Fe and Al oxides and Ca and Mg from the High, Mid and Low field moisture level soils (n = 9 for each moisture level); mean values with standard deviations in parenthesis.

Fe _o (mg kg ⁻¹)			Al _o (mg kg ⁻¹)			Fe _o + Al _o (mg kg ⁻¹)			Ca (mg kg ⁻¹)			Mg (mg kg ⁻¹)		
High	Mid	Low	High	Mid	Low	High	Mid	Low	High	Mid	Low	High	Mid	Low
5408.6 (1082.6)	6543 (1477)	6477 (1095)	2519.9 (597.1) A	1963.2 (366) B	2098.1 (356.1) AB	7927.8 (1430)	8506 (1663)	8566.1 (1424)	2439 (516.1) A	1763.1 (388.4) B	1184.5 (254.4) C	239.1 (48.7) A	155.1 (34) B	108.6 (28.8) C

4. Discussion

4.1. Moisture effects on C mineralization, mineralizability and soil organic carbon

We observed that the wettest field soils displayed lower C mineralizability, even though higher moisture in the laboratory adjusted to the same level as in the field resulted in greater mineralizability. While the former could point towards variation in SOC forms and its stabilization level at higher long-term moisture levels in the field, the latter is a more commonly reported observation (Table S9). In unsaturated soils, increasing water content enables greater solute diffusion to cells, greater microbial viability, and movement in microenvironments. Microbial activity is maximum at a level of moisture where the balance of water and oxygen availability is optimal (Moyano et al., 2013) which is presumably the case at the high moisture levels in our study.

Generally, aerobic microbial activity is optimal at 60% WFPS, with Linn and Doran (1984) reporting highest soil respiration rates between 40 and 70% WFPS, as confirmed by other studies (Table S9). This indicates that even high moisture conditions (63% WFPS) in our experimental setup were well below the range of any anaerobic limitation, indicated by greater laboratory moisture resulting in increased C mineralization and mineralizability, regardless of field moisture (Fig. 1).

Table 5

Summary statistics for fixed effects regarding their effect on C mineralizability (mg C g⁻¹ C) after incubation for 42 days. Model developed to check the influence of field moisture, when controlled for texture components and biomass inputs (shown in italics for p < 0.0001, in bold for p < 0.05).

Effect tests	DF	F Ratio	P value
Field moisture level	2	4.6	0.02
Laboratory moisture level	2	91	< 0.0001
Sand	1	1.8	0.2
Clay	1	1.2	0.3
Cumulative above-ground biomass	1	2.3	0.14
Root biomass (2014)	1	4.1	0.05
PC1	1	14.2	0.0008
PC2	1	0.25	0.62

The average WFPS (63% WFPS) in high moisture field sites occurred in 46% of the monthly field measurements conducted over the four years. The moisture content of these sites was lower than 70% WFPS during 57% of the moisture measurement events and lower than 80% WFPS during 82% of the moisture measurement events over the four years (unpublished data). Therefore, in water adjustments mimicking high field moisture conditions, SOC mineralization was still favored, and any decrease in C mineralizability at higher field moisture was likely not a

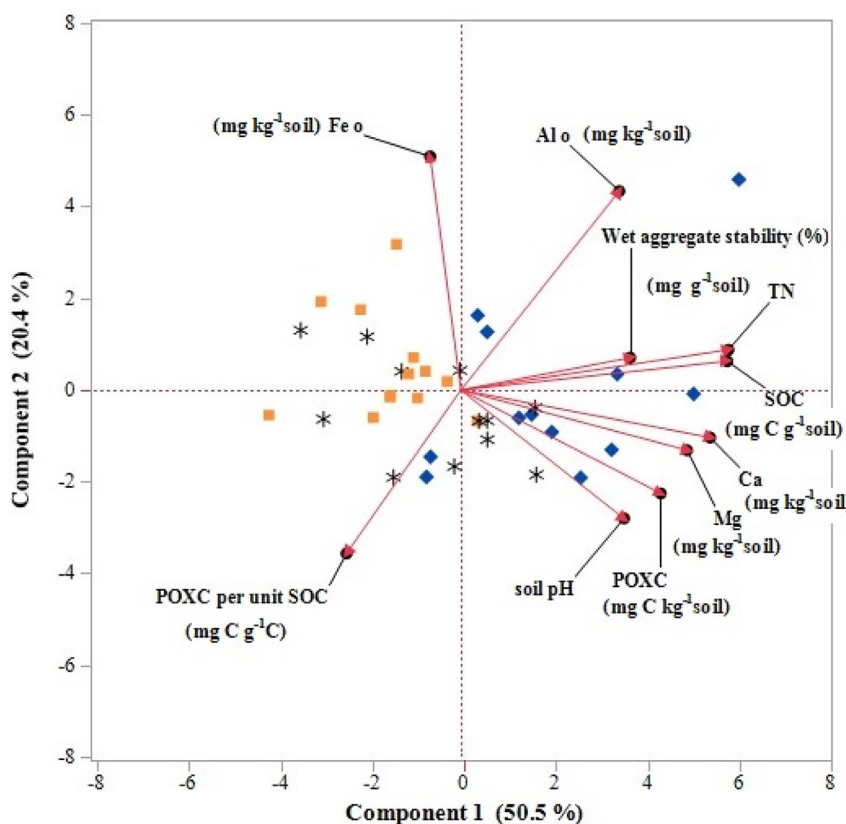


Fig. 4. Biplot of the first two principal components of the variability among soil properties (excluding soil texture components) related to C mineralizability. Red vectors represent principal component loadings of each variable. Blue diamonds, black stars and orange squares represent samples from high, mid, and low field moisture levels, respectively. (For interpretation of the references to colour in this figure legend, the reader is referred to the Web version of this article.)

result of moisture restrictions to mineralization. The lower mineralizability associated with wetter field soils is therefore most likely related to SOC being stabilized differently under wetter conditions.

The greater mean residence time of slow-cycling C pools (MRT_2) in the wettest soils, in comparison to low-moisture soils of each cropping system (Table 3, Table S5d, Table S6) points to a stabilization mechanism for SOC at greater long-term field moisture. Again, the smaller size of the slow-cycling pool (C_2) for the field high-lab high moisture combination soils in comparison to field high-lab low one for any cropping system (Table 3, Table S6) points to our high field moisture level not restricting C mineralization or mineralizability. This stabilization mechanism operates on what is here identified as a slow-mineralizing pool, as fixing the mineralization rate (k_1) of the fast-mineralizing pool to an average value across all moisture levels did not affect the differences in values between slow-cycling pools. This corroborates the interpretation that higher SOC levels were not merely a result of lower mineralization due to unfavorable soil moisture.

The wettest soils in the field experiment had the greatest SOC levels. Of the eighty field subplots present at the site, the thirty-six used in this study show a characteristic trend of greater SOC values (ranging between 26 and 43 mg C g⁻¹ soil) with increasing long-term field moisture. When all eighty subplots were considered, the same OM/SOC trend was seen during each sampling year (2011, 2012, 2013, and 2014), with the wettest soils displaying significantly greater OM and SOC compared to the drier soils (Das et al., 2018). Generally, low biomass C inputs associated with drier soils in the range of soil moistures observed at the study site and greater C inputs associated with higher soil water conditions are thought to result in decreased and increased SOC stocks, respectively. Though litter input measurements had not been included in our study, they can broadly be expected to be proportional to harvested above-ground biomass. As drier soils displayed greater harvested biomass during the preceding growing seasons (Table 2), litter inputs were expected to also be greatest at low water contents in the range occurring at the study site. However, our incubation results indicated that C mineralizability was not correlated to harvested above-ground biomass production and weakly correlated to coarse root biomass (Table 5), and both crop parameters displayed low loading values for principal component analysis with C mineralizability and soil and crop characteristics (Table S8b). Thus, it can be concluded that greater biomass inputs were not a primary reason for lower C mineralizability and hence greater SOC in wetter soils in the field. With high soil moisture not restricting C mineralization at the study site (as shown from our incubation) and with biomass inputs not being the reason for greater SOC, the lower C mineralizability of soils from wetter fields can only be explained by a specific mechanism of SOC stabilization operative in the unsaturated moisture range of the Ap horizon, at neutral/near neutral pH.

4.2. Why was C mineralizability lower in soils of higher long-term water content?

As the lower C mineralizability at higher field moisture was not a result of moisture restrictions to mineralization or of greater biomass inputs, it is most likely related to SOC being stabilized differently under wetter long-term conditions. Low C mineralization may be related to physical protection through aggregation (Six et al., 2000; Six et al., 2002; von Lützow et al., 2006), which limits diffusion of catabolites and enzymes as well as interaction with mineral surfaces (Oades, 1988; Kögel-Knabner et al., 2008; von Lützow and Kögel-Knabner, 2010; Schmidt et al., 2011; Kleber et al., 2015). Greater physical protection through greater aggregation, though important, is less likely the major explanation here; aggregate stability had a weak negative correlation to C mineralizability ($r = -0.2$, $p = 0.03$) and loaded in the same direction (0.61) for PC1 (Fig. 4), which explained 50.5% variability among the soil properties and was significant in explaining differences among C mineralizability (Table 5). It also loaded with a value of 0.53 in PC1*

(Table S8b), which explained 40.9% of the cumulative C mineralizability. The direction and loading value of POXC per unit SOC was -0.4 for PC1 (Fig. 4) as well as for PC1* (Table S8b); its positive correlation with C mineralizability indicated that this parameter was also associated with C mineralizability of the studied soils. POXC per unit SOC represents the amount of readily available, biologically active C pool associated with heavier and smaller particulate organic C fractions (Culman et al., 2012). This fraction that is not associated with minerals is likely used efficiently in heterotrophic respiration and may have been depleted faster in the incubation experiment. Thus, the less-mineralizable SOC that remained was mineral-protected (through organo-mineral interactions and/or aggregations) and resulted in lower mineralizability (in wetter soils) in this experiment.

4.3. Did mineral attachment lead to lower mineralizability of wetter soils?

Greater soil moisture results in increased organic C contained in the soil aqueous phase, which are smaller sized, solvated, mobile molecular fragments which are highly efficient in MOA formation with mineral reactive phases with large specific surface areas, such as Fe oxides, short-range ordered Al-silicates, permanently charged clay minerals or with metal ions (Al^{3+} and Fe^{3+}) via complexation (Eusterhues et al., 2003; Mikutta et al., 2005; Kalbitz and Kaiser, 2008; Kleber et al., 2015). Increased heterotrophic respiration (and to some extent root respiration) in wetter soils can lead to a decrease in soil pH which creates secondary minerals resulting in increased formation of MOAs through processes of adsorption and coprecipitation (Kleber et al., 2015). While low pH of the soil solution leads to stronger innerspace bonds between metal oxides and clay minerals, weaker outerspace complexation and H-bonds are active at neutral and alkaline pH (Kleber et al., 2015). The low C mineralizability of such soils near neutral pH is an important reason why adsorption is not thought to be the sole reason for long turnover times of OM (Torn et al., 2009). While coprecipitation is a driving mechanism of OM stabilization in wet anaerobic soil systems (where reduced Fe (II) in soil solution is oxidized to Fe (III) upon aeration and then coprecipitates with OM), such a mechanism can also be prevalent in upland soils exposed to partial anaerobic conditions (Fimmen et al., 2007; Thompson et al., 2006; Kleber et al., 2015), especially in the rhizosphere region (Collignon et al., 2012; Kleber et al., 2015). For our field soils (pH range 5.1–6.3), mechanisms of stabilization common for circumneutral/mildly acidic exposed to partial oxygen deficiency conditions during hydrological events are therefore possible. Additionally, organic matter composition and its effects on sorption or coprecipitation may also dictate MOA formation, with O/N-alkyl C, alkyl C, aromatic C, carboxyl C moieties displaying selective preferences (Kleber et al., 2015). Additionally, as OM bound via weaker electrostatic forces display greater desorption in comparison to innerspace complexes (Mikutta et al., 2007; Wang and Lee, 1993), it can also be proposed to be a mechanistic explanation in our experiment, where C stabilization is best explained by outerspace weak bonding in the neutral/near neutral pH range. Therefore, an influence of long-term moisture on the distribution of secondary minerals and any such MOA formation mechanism could contribute to explain the decreased C mineralizability of the wetter field soils in our experiment.

As bulk soil Fe_o levels were found not to vary among the soils of differing long-term field moisture contents, we were not able to conclusively posit Fe_o as a reason for the observed lower C mineralizability in the wettest soils. Additionally, we could not ascribe the lower C mineralizability of the wetter soils to Al, as Al_o levels of the high moisture soils were not significantly greater than low moisture soils (although they were significantly greater than in the mid moisture soils). As C mineralizability displayed good correlation with Al_o ($r = -0.55$, $p < 0.0001$) and Al_o loaded well in the same direction (0.57) for PC1 (Fig. 4), which explained 50.5% variability among the soil properties and was significant in explaining differences among C mineralizability (Table 4), we believe that Al_o possibly played some role

in decreased mineralizability in our experiment. Insoluble Al-OM complexes have already been described as a major pathway for the formation of persistent soil OM (Scheel et al., 2007; Hernández-Soriano, 2012).

However, the significantly greater Ca and Mg presence in the high moisture soils from our experiment, in comparison to both the mid and low moisture soils (Table 4) provided compelling evidence in favor of involvement of these two polyvalent cations in a long-term SOC stabilization mechanism in these soils which resulted in significantly low C mineralizability. As the pH (varying between 5.1 and 6.3) of the soils in our experiment were near neutral, we believe that Ca- and Mg-mediated OM stabilization may have played an important role. Hence both inner- and outer-sphere bridging by Ca^{2+} is potentially an important strategy for SOC stabilization. A strong correlation with increased adsorption of extracellular polymeric substances to clays in the presence of divalent Ca ions has also been reported (Newcomb et al., 2017). In a study by Chen and Sparks (2015), close spatial SOM-Ca associations were found in anoxic wetland soils free from Fe oxides.

Ca-mediated aggregation and soil structural stability improvements are well known (Kayler et al., 2011; Rowley et al., 2018) and are thought to impact the SOC accrual potential of soils. The positive relationship between aggregate stability and C mineralizability measured in our experiment is consistent with this mechanism. As our study only evaluated aggregates between 250 and 2000 μm in diameter, stabilization mechanisms related to sub-micron scale aggregation and chemical stabilization on mineral surfaces remain to be investigated.

Some reasons of extensive presence of Ca^{2+} within surface soil are weathering of rocks or surface formations, anthropogenic inputs, or lateral/upward movement of Ca^{2+} water. As the amount of exchangeable Ca and Mg were higher in the wettest soils than in the lower moisture groups, processes of organo-mineral complexation, erosion, deposition, or shallow groundwater flow may explain the differences in stabilization. There is strong possibility of the seasonally saturated and poorly drained conditions of the wettest soils might have led to upward migration of Ca^{2+} and Mg^{2+} from a calcareous parent material. The poorly drained Madalin and related Dalton and Canaseraga soil series have carbonate presence beyond 0.6 m (Neeley, 1965; Cline and Bloom, 1965). Our work in related study (Das, 2017) involving a subset of soils from depths between 0.6 and 1.2 m from the same field confirmed carbonate presence as evidenced by effervescence with 5 M HCl.

5. Conclusion

In our experiment, added moisture increased C mineralizability in the tested moisture range, indicating that greater moisture during incubation resulted in increased rates of aerobic heterotrophic respiration. However, wetter field soils in the same range displayed decreased C mineralizability with longer mean residence time of the slow-mineralizing C pools, suggesting a mineral-associated pathway of OM stabilization operative in the wetter soils in comparison to drier ones. Climate-carbon cycle feedback is intricately related to SOC response to moisture. However, most SOC models, such as CENTURY (Parton et al., 1987) or RothC (Coleman and Jenkinson, 1999), typically assume greater mineralization and do not consider greater stabilization with wetter ambient conditions. Multiple moisture-driven abiotic and biotic factors operative in surface soils are likely to control mineral-related SOC stabilization. Integrating microbial community and extracellular enzyme studies, controlled field respiration studies, and analytical approaches characterizing MOAs to such long-term incubation experiments will substantially solidify results and help with expounding the mechanistic processes surrounding moisture and mineral associated SOC stabilization.

Acknowledgements

This research was supported by the Sustainable Bioenergy Program

Grant No. 2011-67009-20083 from the USDA National Institute of Food and Agriculture, and by the Federal Capacity (Hatch) Project No. NYC-123486 awarded through Cornell University's College of Agriculture and Life Sciences. The authors are extremely thankful to all project assistants and summer interns of the Projects for their help and support. Many thanks to Maria Gannet and Akio Enders for their kind help. Thanks to everybody at the Lehmann lab. Thanks to Teamrat A. Ghezzei, UC Merced for help with curve fitting procedure with R code. The work also could not be completed without the help of Kevin Packard and Francoise Vermeylen of the Cornell Statistical Computing Unit, Cornell University.

Appendix A. Supplementary data

Supplementary data to this article can be found online at <https://doi.org/10.1016/j.soilbio.2018.12.006>.

References

- Bonin, C.L., Lal, R., 2014. Aboveground productivity and soil carbon storage of biofuel crops in Ohio. *Global Change Biology Bioenergy* 6, 67–75.
- Chen, C., Sparks, D.L., 2015. Multi-elemental scanning transmission X-ray microscopy–near edge X-ray absorption fine structure spectroscopy assessment of organo-mineral associations in soils from reduced environments. *Environmental Chemistry* 12, 64–73.
- Chenu, C., Plante, A.F., 2006. Clay-sized organo-mineral complexes in a cultivation chronosequence: revisiting the concept of the “primary organo-mineral complex”. *European Journal of Soil Science* 57, 596–607.
- Cline, M.G., Bloom, A.L., 1965. Soil Survey of Cornell University Property and Adjacent Areas. New York State College of Agriculture at Cornell University, Ithaca.
- Coleman, K., Jenkinson, D.S., 1999. RothC-26.3, a Model for the Turnover of Carbon in Soil: Model Description and User's Guide, Lawes Agric. Trust, Harpenden, U. K.
- Collignon, C., Ranger, J., Turpault, M.P., 2012. Seasonal dynamics of Al- and Fe-bearing secondary minerals in an acid forest soil: influence of Norway spruce roots (*Picea abies* (L.) Karst.). *European Journal of Soil Science* 63 (5), 592–602.
- Culman, S.W., Snapp, S.S., Freeman, M.A., Schipanski, M.E., Beniston, J., Lal, R., Drinkwater, L.E., Franzluebbers, A.J., Glover, J.D., Grandy, A.S., Lee, J., Six, J., Maul, J.E., Mirksy, S.B., Spargo, J.T., Wander, M.M., 2012. Permanganate oxidizable carbon reflects a processed soil fraction that is sensitive to management. *Soil Science Society of America Journal* 76 (2), 494–504.
- Das, S., 2017. Soil Carbon Dynamics in Wetness-prone Marginal Soils under Perennial Grass Bioenergy Crops of Northeastern United States. PhD Thesis. Cornell University, USA.
- Das, S., Teuffer, K., Stoof, C.R., Walter, M.T., Walter, M.F., Steenhuis, T.S., Richards, B.K., 2018. Perennial grass bioenergy cropping on wet marginal land: impacts on soil properties, soil organic carbon, and biomass during initial establishment. *BioEnergy Research* 11, 262–276.
- Eusterhues, K., Rumpel, C., Kleber, M., Kögel-Knabner, I., 2003. Stabilization of soil organic matter by interactions with minerals as revealed by mineral dissolution and oxidative degradation. *Organic Geochemistry* 34, 1591–1600.
- Fimmen, R.L., Cory, R.M., Chin, Y.-P., Trouts, T.D., McKnight, D.M., 2007. Probing the oxidation–reduction properties of terrestrially and microbially derived dissolved organic matter. *Geochimica et Cosmochimica Acta* 71 (12), 3003–3015.
- Fornara, D.A., Steinbeiss, S., McNamara, N.P., Gleixner, G., Oakley, S., Poulton, P.R., Macdonald, A.J., Bardgett, R.D., 2011. Increases in soil organic carbon sequestration can reduce the global warming potential of long-term liming to permanent grassland. *Global Change Biology* 17, 1925–1934.
- Hernández-Soriano, M.C., 2012. The role of aluminum-organosilicates in soil organic matter dynamics. In: Hernández-Soriano, M.C. (Ed.), *Soil Health and Land Use Management*. InTech, 978-953-307-614-0, pp. 17–32.
- Jarrell, W.M., Armstrong, D.E., Grigal, D.F., Kelley, E.F., Monger, H.C., Wedin, D.A., 1999. Soil water and temperature status. In: Robertson, G.P., Coleman, D.C., Bledsoe, C.S., Sollins, P. (Eds.), *Standard Soil Methods for Long-term Ecological Research*. Oxford University Press, New York, NY, pp. 55–73.
- Jobbágy, E.G., Jackson, R.B., 2000. The vertical distribution of soil organic carbon and its relation to climate and vegetation. *Ecological Applications* 10, 423–436.
- Kalbitz, K., Kaiser, K., 2008. Contribution of dissolved organic matter to carbon storage in forest mineral soils. *Journal of Plant Nutrition and Soil Science* 171, 52–60.
- Kayler, Z.E., Kaiser, M., Gessle, R.A., Ellerbrock, R.H., Sommer, M., 2011. Application of delta C-13 and delta N-15 isotopic signatures of organic matter fractions sequentially separated from adjacent arable and forest soils to identify carbon stabilization mechanisms. *Biogeochemistry* 8 (10), 2895–2906.
- Kemmitt, S.J., Lanyon, C.V., Waite, I.S., Wen, Q., Addiscott, T.M., Bird, N.R.A., O'Donnell, T., Brookes, P.C., 2008. Mineralization of native soil organic matter is not regulated by the size, activity or composition of the soil microbial biomass—a new perspective. *Soil Biology and Biochemistry* 40, 61–73.
- Kirschbaum, M.U.F., 2006. The temperature dependence of organic-matter decomposition – still a topic of debate. *Soil Biology and Biochemistry* 38, 2510–2518.
- Kleber, M., Mikutta, R., Torn, M.S., Jahn, R., 2005. Poorly crystalline mineral phases protect organic matter in acid subsoil horizons. *European Journal of Soil Science* 56,

- 717–725.
- Kleber, M., Eusterhues, K., Keilweil, M., Mikutta, C., Mikutta, R., Nico, P.S., 2015. Mineral-organic associations: formation, properties, and relevance in soil environments. *Advances in Agronomy* 130, 1–140.
- Kögel-Knabner, I., Guggenberger, G., Kleber, M., Kandeler, E., Kalbitz, K., Scheu, S., Eusterhues, K., Leinweber, P., 2008. Organo-mineral associations in temperate soils: integrating biology, mineralogy, and organic matter chemistry. *Journal of Plant Nutrition and Soil Science* 171, 61–82.
- Lehmann, J., Kleber, M., 2015. The contentious nature of soil organic matter. *Nature* 528, 60–68.
- Liang, B., Lehmann, J., Solomon, D., Sohi, S., Thies, J.E., Skjemstad, J.O., Luizao, F.J., Engelhard, M.H., Neves, E.G., Wirrick, S., 2008. Stability of biomass-derived black carbon in soils. *Geochimica et Cosmochimica Acta* 72, 6069–6078.
- Linn, D.M., Doran, J.W., 1984. Aerobic and anaerobic microbial populations in no-till and plowed soils. *Soil Science Society of America Journal* 48, 794–799.
- Mason, C.W., Stoof, C.R., Richards, B.K., Das, S., Goodale, C.L., Steenhuis, T.S., 2017. Hotspots of nitrous oxide emission in fertilized and unfertilized perennial grasses on wetness-prone marginal land in New York State. *Soil Science Society of America Journal* 81, 452–458.
- McKeague, J.A., Day, J.H., 1966. Dithionite and oxalate Fe and Al as aids in differentiating various classes of soils. *Canadian Journal of Soil Science* 46, 13–22.
- Mikutta, R., Kleber, M., Jahn, R., 2005. Poorly crystalline minerals protect organic carbon in clay subfractions from acid subsoil horizons. *Geoderma* 128, 106–115.
- Mikutta, R., Mikutta, C., Kalbitz, K., Scheel, T., Kaiser, K., Jahn, R., 2007. Biodegradation of forest floor organic matter bound to minerals via different binding mechanisms. *Geochimica et Cosmochimica Acta* 71, 2569–2590.
- Moebius-Clune, B.N., Moebius-Clune, D.J., Gugino, B.K., Idowu, O.J., Schindelbeck, R.R., Ristow, A.J., van Es, H.M., Thies, J.E., Shayler, H.A., McBride, M.B., Wolfe, D.W., Abawi, G.S., 2016. Comprehensive assessment of soil health. In: *The Cornell Framework Manual*, third ed. Cornell University, Geneva, United States, pp. 51–52.
- Moyano, F., Manzoni, S., Chenu, C., 2013. Responses of soil heterotrophic respiration to moisture availability: an exploration of processes and models. *Soil Biology and Biochemistry* 59, 72–85.
- Neeley, J.A., 1965. Soil Survey, Tompkins County, New York. United States Department of Agriculture, Soil Conservation Service in cooperation with Cornell University Agriculture Extension Station. pp. 25 Series 1961.
- O'Brien, S.L., Jastrow, J.D., Grimley, D.A., Gonzalez-Meler, M.A., 2015. Edaphic controls on soil organic carbon stocks in restored grasslands. *Geoderma* 251–252, 117–123.
- Oades, J.M., 1988. The retention of organic matter in soils. *Biogeochemistry* 5, 35–70.
- Parton, W.J., Schimel, D.S., Cole, C.V., Ojima, D.S., 1987. Analysis of factors controlling soil organic matter levels in Great Plains grasslands. *Soil Science Society of America Journal* 51, 1173–1179.
- Porras, R.C., Hicks Pries, C.E., McFarlane, K.J., Hanson, P.J., Torn, M.S., 2017. Association with pedogenic iron and aluminum: effects on soil organic carbon storage and stability in four temperate forest soils. *Biogeochemistry* 133, 333–345.
- Propheter, J.L., Staggenborg, S.A., 2010. Performance of annual and perennial biofuel crops: nutrient removal during the first two years. *Agronomy Journal* 102, 798–805.
- R Studio Team, 2015. RStudio. Integrated Development for R. RStudio, Inc., Boston, MA.
- Richards, B.K., Stoof, C.R., Mason, C., Crawford, R.V., Das, S., Hansen, J.L., Mayton, H.S., Crawford, J.L., Steenhuis, T.S., Walter, M.T., Viands, D.R., 2013. Carbon Sequestration and Gaseous Emissions in Perennial Grass Bioenergy Cropping Systems in the Northeastern US. AAIC Proceedings, Washington DC.
- Richards, B.K., Stoof, C.R., Cary, I.J., Woodbury, P.B., 2014. Reporting on marginal lands for bioenergy feedstock production - a modest proposal. *BioEnergy Research* 7, 1060–1062.
- Rowley, M.C., Grand, S., Verrecchia, É.P., 2018. Calcium-mediated stabilisation of soil organic carbon. *Biogeochemistry* 137, 27–49.
- Scheel, T., Dörfler, C., Kalbitz, K., 2007. Precipitation of dissolved organic matter by aluminum stabilizes carbon in acidic forest soils. *Soil Science Society of America Journal* 71 (1), 64–74.
- Schmidt, M.W.I., Torn, M.S., Abiven, S., Dittmar, T., Guggenberger, G., Janssens, I., Kleber, M., Kögel-Knabner, I., Lehmann, J., Manning, D.A.C., Nannipieri, P., Rasse, D.P., Weiner, S., Trumbore, S., 2011. Persistence of soil organic matter as an ecosystem property. *Nature* 478, 49–56.
- Schwertmann, U., 1964. Differenzierung der Eisenoxide des Bodens durch Extraktion mit Ammoniumoxalatlösung. *Zeitschrift für Pflanzenernährung und Bodenkunde* 105, 194–202.
- Six, J., Elliott, E.T., Paustian, K., 2000. Soil macroaggregate turnover and microaggregate formation: a mechanism for C sequestration under no-tillage agriculture. *Soil Biology and Biochemistry* 32, 2099–2103.
- Six, J., Conant, R.T., Paul, E.A., Paustian, K., 2002. Stabilization mechanisms of soil organic matter: implications for C-saturation of soils. *Plant and Soil* 241, 151–176.
- Sposito, G., Lund, L.J., Chang, A.C., 1982. Trace metal chemistry in arid-zone field soils amended with sewage sludge: I. Fractionation of Ni, Cu, Zn, Cd, and Pb in Solid Phases. *Soil Science Society of America Journal* 46, 260–264.
- Steenhuis, T.S., Winchell, M., Rossing, J., Zollweg, J.A., Walter, M.F., 1995. SCS runoff equation revisited for variable source runoff areas. *Journal of Irrigation and Drainage Engineering* 121, 234–238.
- Stockmann, U., Adams, M.A., Crawford, J.W., Field, D.J., Henakaarchchi, N., Jenkins, M., Minasny, B., McBratney, A.B., de Remy de Courcelles, V., Singh, K., Wheeler, I., Abbott, L., Angers, D.A., Baldock, J., Bird, M., Brookes, P.C., Chenu, C., Jastrow, J.D., Lal, R., Lehmann, J., O'Donnell, A.G., Parton, W.J., Whitehead, D., Zimmermann, M., 2013. The knowns, known unknowns and unknowns of sequestration of soil organic carbon. *Agriculture, Ecosystems & Environment* 164, 80–99.
- Thompson, A., Chadwick, O.A., Rancourt, D.G., Chorover, J., 2006. Iron-oxide crystallinity increases during soil redox oscillations. *Geochimica et Cosmochimica Acta* 70, 1710–1727.
- Tipping, E., 2005. Modelling Al competition for heavy metal binding by dissolved organic matter in soil and surface waters of acid and neutral pH. *Geoderma* 127 (3–4), 293–304.
- Torn, M.S., Trumbore, S.E., Chadwick, O.E., Vitousek, P.M., Hendricks, D.M., 1997. Mineral control of soil organic carbon storage and turnover. *Nature* 389, 170–173.
- Torn, M.S., Swanston, C.W., Castanha, C., Trumbore, S.E., 2009. Storage and turnover of organic matter in soil. In: Senesi, N., Xing, B., Huang, P.M. (Eds.), *Biophysico-chemical Processes Involving Natural Nonliving Organic Matter in Environmental Systems*. John Wiley & Sons, Inc, Hoboken, New Jersey, pp. 219–272.
- Trumbore, S.E., 1997. Potential responses of soil organic carbon to global environmental change. *Proceedings of the National Academy of Sciences U.S.A.* 94, 8284–8291.
- von Lützw, M., Kögel-Knabner, I., 2010. Response to the concept paper: "what is recalcitrant soil organic matter?" by Markus Kleber. *Environmental Chemistry* 7, 333–335.
- von Lützw, M., Kögel-Knabner, I., Ekschmitt, K., Matzner, E., Guggenberger, G., Marschner, B., Flessa, H., 2006. Stabilization of organic matter in temperate soils: mechanisms and their relevance under different soil conditions - a review. *European Journal of Soil Science* 57, 426–445.
- Walter, M.T., Walter, M.F., Brooks, E.S., Steenhuis, T.S., Boll, J., Weiler, K.R., 2000. Hydrologically sensitive areas: variable source area hydrology implications for water quality risk assessment. *Journal of Soil & Water Conservation* 3, 277–284.
- Wang, X.C., Lee, C., 1993. Adsorption and desorption of aliphatic amines, amino acids and acetate by clay minerals and marine sediments. *Marine Chemistry* 44 (1), 1–23.
- Weil, R.R., Islam, K.R., Stine, M.A., Gruver, J.B., Sampson-Liebig, S.E., 2003. Estimating active carbon for soil quality assessment; a simplified method for laboratory and field use. *American Journal of Alternative Agriculture* 18, 3–17.
- Whitman, T., Zhu, Z., Lehmann, J., 2014. Carbon mineralizability determines interactive effects on mineralization of pyrogenic organic matter and soil organic carbon. *Environmental Science & Technology* 48 (23), 3727–3734.
- Zimmerman, A., Gao, B., Ahn, M.Y., 2011. Positive and negative mineralization priming effects among a variety of biochar-amended soils. *Soil Biology and Biochemistry* 43, 1169–1179.
- Zollweg, J.A., Gburek, W.G., Steenhuis, T.S., 1996. SmoRMod - a GIS-integrated rainfall runoff model. *Transactions of the American Society of Agricultural Engineers* 39, 1299–1307.